www.amlett.com, www.vbripress.com/aml, DOI: 10.5185/amlett.2015.5725 Published online by the VBRI press in 2015

Ion irradiation induced crystallization in iron phosphate glass – TEM investigations

P. Jegadeesan[1], S. Amirthapandian[1*], Kitheri Joseph[2], C. David[1], B.K. Panigrahi[1], K.V. G Kutty[2]

[1]*Materials Physics Division, Materials Science Group, Indira Gandhi Centre for Atomic Research, Kalpakkam 603 102, India*
[2]*Materials Chemistry Division, Chemistry Group, Indira Gandhi Centre for Atomic Research, Kalpakkam 603 102, India*

[*]Corresponding author. Tel: (+91) 44 27480081; E-mail: pandian@igcar.gov.in

Received: 28 August 2014, Revised: 18 November 2014 and Accepted: 08 December 2014

ABSTRACT

Iron phosphate glass (IPG) is considered as a suitable matrix for the immobilization of nuclear waste containing higher concentration of Cs, rare earth, Mo and Cr. The central issue, while disposing nuclear waste in glass matrices, is the damage in glass matrices due to the ballistic processes caused by atomic displacements due to α-particles and the recoiling of heavy nuclei resulting from actinide decay. Ion irradiation produces similar kind of damage, and hence the samples are irradiated with 4 MeV O^+ (self) ion. The microstructural studies were carried out using transmission electron microscopy (TEM) for as-prepared, annealed and ion irradiated samples. It is observed that ion irradiation in IPG leads to the formation of nanocrystals with different phases containing Fe, P and O. Thermally activated crystallization process is ruled out based on the non-equilibrium experimental conditions. In the present experiments, stress driven crystallization mechanism was invoked. The stress, around the ion track formed during ion irradiation, is larger than the yield strength of the glass and hence, the surrounding matrix undergoes substantial deformation resulting in the formation of shear bands. Nucleation of nanocrystals is driven by the stress in the vicinity of the shear bands. Copyright © 2015 VBRI press.

Keywords: Iron phosphate glass; ion irradiation; electron microscopy; crystallization.

P. Jegadeesan is working as Scientific Officer in Materials Science Group, Indira Gandhi Centre for Atomic Research, Kalpakkam. Currently he is working towards doctoral degree at Homi Bhabha National Insitute (HBNI), India. His research interests are experiments and simulations on radiation damage in materials.

S. Amirthapandian received his Ph.D. degree from University of Madras in 2004. Currently, he is working as Scientific Officer at Indira Gandhi Centre for Atomic Research, India. He worked as a postdoctoral researcher, during 2008-10, in the University of Stuttgart, Germany. His current research interests are radiation damage in nuclear materials and micro-structural study on materials. He is Assistant Professor at Homi Bhabha National Insitute (HBNI), India.

B.K. Panigrahi received his Ph.D. from Indian Institute of Science, Bangalore. Currently he is heading both Accelerator Materials Science Section and Computational Materials Science Section in Indira Gandhi Centre for Atomic Research. His research interests are radiation damage simulations, void swelling in reactor structural materials and ion irradiation effects on nanomaterials. He is professor at Homi Bhabha National Institute (HBNI), India.

Introduction

The aqueous high level waste (HLW) originating from fast reactors is largely different from that of thermal reactors. The HLW from fast reactors consists of minor actinides, noble metals volatile fission products and rare earths in higher concentrations compared to the HLW from thermal reactors. While borosilicate glass (BSG) is the well known matrix for the immobilization of the HLW arising after reprocessing the spent fuel from thermal reactors **[1]**, iron phosphate glass (IPG) is considered as a suitable alternate matrix for the immobilization of high level nuclear waste from fast reactors. It is observed that the structural and the thermal characteristics of IPG remain largely unaltered, by the addition of upto 20 wt% of simulated fast reactor waste **[2]**.

The main problem in disposing HLW in glass matrices is the damage caused by the energetic α-particles and the recoiling heavy nuclei resulting from actinide decay. However, very few reports are available regarding radiation damage studies on IPG. Many reports are available on radiation damage studies on silicon based glasses **[3]** but that cannot be extrapolated to phosphate glasses. It is mainly because of the fundamental difference in the chemical nature of the two glasses; silicate glasses are based on 4-corner sharing tetrahedral network, whereas

phosphate glasses are generally 3-corner sharing tetrahedral network.

Sun *et al*. [4] have reported the effects of electron beam and ion beam irradiations on IPG. Electron beam irradiation leads to the formation of Fe-rich and pure P phases whereas the ultra low energy (3.5 keV Ar^+) ion irradiation on IPG leads to the formation of Fe/FeO nanoparticles as a result of preferential sputtering during ion irradiation, i.e., P and O were sputtered out at a higher rate than Fe. Awazu et al. **[5]** have reported that swift heavy ion irradiation on zinc phosphate glass shows the formation of ion tracks and leads to reduction in the number of bridging O atoms.

In the present work, the stability of the glass nature of IPG under ion irradiation (4 MeV O^+ ions) is studied for the first time. In order to rule out the role of impurity atoms, irradiation was carried out with self-ions (O^+ ions). TEM studies confirmed that ion irradiation induced crystallization has taken place in the specimen. The crystallization mechanism is discussed in the light of thermal spike process.

Experimental

Materials

Iron Phosphate Glass (IPG) samples were prepared by mixing Fe_2O_3 (Alfa Aesar, 99.5% purity) and ADP (ammonium dihydrogen phosphate - $NH_4H_2PO_4$) (Merck, 99% purity) maintaining Fe/P atomic ratio as 0.67. The mixture was calcined at 673 K in Pt crucible for 1½ hour in order to facilitate the decomposition of ADP. The calcined material was melted and quenched in air at 1423 K to obtain IPG sample **[6]**.

Method

IPG samples were irradiated with 4 MeV O^+ ions at room temperature using 1.7 MV Tandetron Accelerator. Ion irradiation was carried out for different ion fluences ranging from 5×10^{13} ions/cm^2 to 5×10^{16} ions/cm^2. In order to compare the effect of ion irradiation and the effect of temperature on crystallization process, we have heat treated the IPG sample at 900 °C for 48 hours in ambient atmosphere. The crystallization temperature was chosen based on Ref. **[6]**. SRIM calculations **[7]** show that the projected range of 4 MeV O^+ ions in IPG is 3.8 µm with a straggling of 283 nm.

The as prepared, the ion irradiated and the heat treated IPG samples were studied using LIBRA 200FE, a high resolution transmission electron microscope (HRTEM). The surface of the as-prepared/irradiated/heat-treated IPG sample was scratched with scalpel blade and the scratched specimen was collected on a TEM-grid by keeping the grid on the scratched region and drop casting isopropyl alcohol. The grid was dried and then observed under transmission electron microscope.

The HRTEM is operated at 200 kV and it is equipped with Schottky field emission gun (FEG) and an in-column omega energy filter. The information limit of the microscope is 0.13 nm and the energy resolution for EELS is 0.7 eV. Electron diffraction patterns, HRTEM images and electron energy loss spectra were recorded from the TEM and the images were analysed using ImageJ software **[8]**.

Results and discussion

Fig. 1 shows the selected area electron diffraction (SAED) patterns obtained from the as-prepared, the ion irradiated and the heat treated IPG samples. The *d*-values identified in the SAED patterns of each sample are compared with all the possible phases containing Fe, P and O, reported in ICDD database.

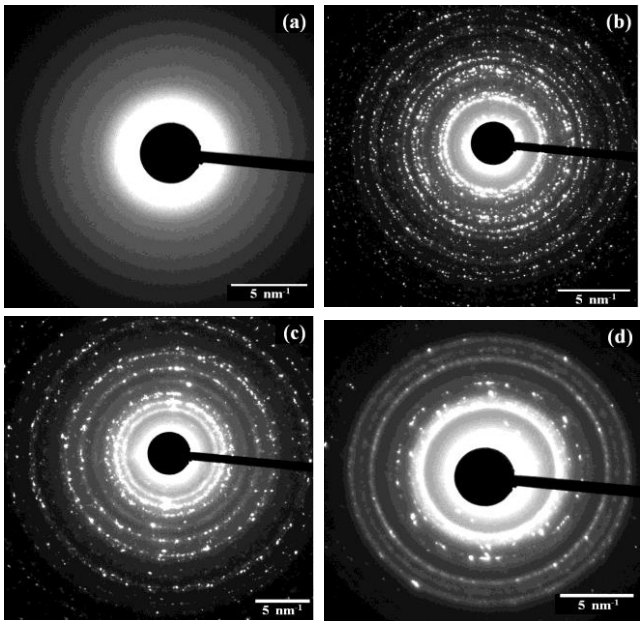

Fig. 1. The selected area electron diffraction patterns of (a) as prepared IPG sample, (b) sample heat treated at 900 °C for 48 hrs, sample irradiated with O^+ up to an ion fluence of (c) 5×10^{13} ions/cm^2 and (d) 5×10^{16} ions/cm^2. Spotty rings confirm the presence of nanocrystals. The identified *d* spacings are given in Table. 1.

The SAED pattern from the as-prepared IPG sample (**Fig. 1a**) shows the hollow rings which are typical for an amorphous solid. The intensity of the broad ring peaks at a radial distance corresponding to ~4.08 Å. This is close to the value of short range order in IPG glass as deduced from the amorphous background in the XRD data **[6]**. The spotty rings in the SAED pattern of the heat treated IPG sample **(Fig. 1b)** confirm the presence of nanocrystalline phases in the sample. The diffraction rings were indexed to the two phases $Fe_4(P_2O_7)_3$ and $Fe(PO_3)_3$ (JCPDS# 04-010-4482 and 89-8524 respectively). The matching *d*-values of the above phases are listed in **Table. 1**. Kitheri et al. **[6]** have reported that $Fe_3(P_2O_7)_2$, $Fe_4(P_2O_7)_3$ and $Fe(PO_3)_3$ phases are seen in the IPG sample heat treated in Ar atmosphere. The absence of $Fe_3(P_2O_7)_2$ phase in the present study could be due to the difference in the heat treatment atmosphere. However, another report **[9]** states that IPG glass with Fe/P atomic ratio 0.67 is expected to undergo predominantly an eutectic phase transition at 907 °C and crystallize into $Fe_4(P_2O_7)_3$ and $Fe(PO_3)_3$. Alternatively it may undergo congruent melting and form the crystalline phase $Fe_4(P_2O_7)_3$ at 945 °C.

Fig. 1(c) and **Fig. 1(d)** shows the SAED patterns of the IPG samples irradiated with O^+ ion up to two different ion

fluences 5×10^{13} ions/cm^2 and 5×10^{16} ions/cm^2 respectively. Both the samples have spotty rings in the electron diffraction patterns indicating the presence of nanocrystalline phases. This shows that ion irradiation has led to crystallization in IPG. The *d* values observed in the diffraction patterns of both the irradiated samples are given in **Table. 1**. The diffraction pattern for the sample irradiated up to an ion fluence of 5×10^{13} ions/cm^2 matches with $Fe_4(P_2O_7)_3$, $Fe(PO_3)_3$ and P_2O_5 phases, whereas the sample with the ion fluence of 5×10^{16} ions/cm^2 shows the presence of $Fe_4(P_2O_7)_3$ and P_2O_5 phases.

Table. 1 Comparison of d-spacing (in Å) of the heat treated and the ion irradiated IPG samples with JCPDS database.

Sample	*d*-spacing (Expt) Å	$Fe_4(P_2O_7)_3$ (04-010-4482) Å (*hkl*)	$Fe(PO_3)_3$ (898524) Å (*hkl*)	P_2O_5 (750389) Å (*hkl*)
Heat treated IPG	4.77		4.65	
	3.01	3.03 (240)	2.71 (132)	
	2.71	2.72 (043)	2.43 (202)	
	2.44	2.44 (310)	1.92 (332)	
	1.92	1.92 (234)	1.61 (442)	
	1.61	1.61 (245)	1.52	
	1.50			
5×10^{13} ions/cm^2	2.24	2.25 (034)	2.24	
	1.83	1.83 (115)	1.83	1.61 (232)
	1.61	1.61 (245)	1.61	1.25 (351)
	1.26			1.16 (523)
	1.16			
5×10^{16} ions/cm^2	2.87	2.89 (212)		
	2.28	2.28 (233)		1.95 (231)
	1.96	1.96 (224)		1.67 (240)
	1.67	1.67 (274)		1.40 (531)
	1.40			1.18 (160)
	1.18			

Fig. 2(a) shows the HRTEM image of the as-prepared IPG sample. It clearly shows the amorphous (glassy) nature of the IPG sample. The amorphous nature is also obvious from the fast Fourier transform (FFT) image (inset) which does not show any spots. **Fig. 2(b)** shows the TEM image of the heat treated IPG sample. The FFT is calculated in the highlighted region of **Fig. 2(b)**, and the inverse fast Fourier transform (IFFT) image (inset) is generated after filtering the noise. The *d* values are measured from the IFFT image and found to be 3.49 Å and 5.09 Å. These *d* values match with the set of planes (132) and (121) of $Fe_4(P_2O_7)_3$ respectively. The HRTEM image of the IPG sample irradiated with 4MeV O^+ up to an ion fluence of 5×10^{13} ions/cm^2 is shown in **Fig. 2(c)** and it clearly shows the presence of lattice fringes in the amorphous background. The *d* values are found to be 3.72 Å and 3.84 Å and these *d* values match with (122) and (051) planes of $Fe_4(P_2O_7)_3$ respectively. The average crystallite size is calculated from the dark field images (not given) and it is found to be 7.0 nm. **Fig. 2(d)** shows the IPG sample irradiated with O^+ ion up to a fluence of 5×10^{16} ions/cm^2. The FFT is calculated in the highlighted region of **Fig. 2(d)**, the noise is filtered and the inverse fast Fourier transform (IFFT) image is calculated (inset). The *d* value 2.09Å matches with that of (332) planes of $Fe_4(P_2O_7)_3$. All the high resolution bright field images in **Fig. 2** were recorded from the region of the sample where the presence of Fe, P and O was confirmed with electron energy loss spectra.

In summary, it is found that 4 MeV O^+ ion irradiation on IPG has led to the formation of nanocrystalline phases with Fe, P and O. It is observed that crystallization takes place even at low ion fluence, however, the size of the nanocrystals increases with the ion fluence.

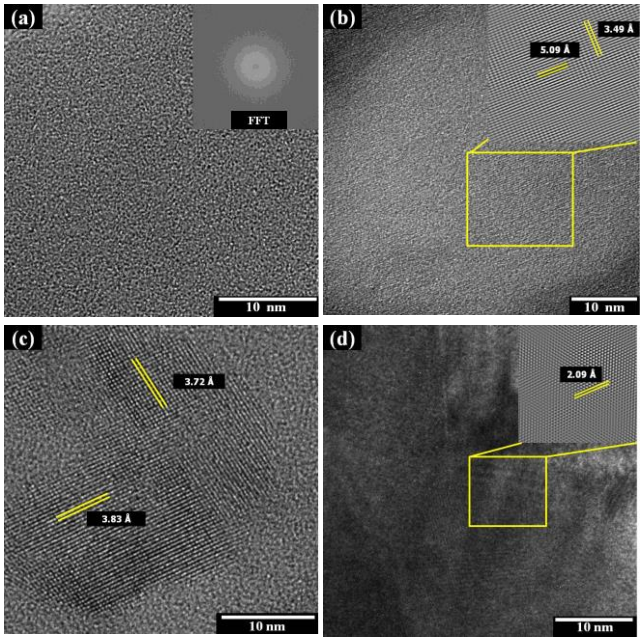

Fig. 2. TEM high resolution images from (a) as prepared IPG sample, (b) sample heat treated at 900 °C for 48 hrs, (c) sample irradiated with O^+ up to a fluence of 5×10^{13} ions/cm^2 and (d) sample irradiated with O^+ up to a fluence of 5×10^{16} ions/cm^2.

Crystallization of an amorphous solid is a complex process. In general, the amorphous to crystalline phase transformation is activated by thermal energy of the system. The overall activation energy for the crystallization of an iron phosphate glass obtained by Kissinger method is 3.29 eV/atom **[10]** which corresponds to a very high temperature (of the order of 10^4 K). Similarly, the critical cooling rate for IPG is ~10 K/s **[11]** which is much smaller compared to metallic glasses where the critical cooling rates are of the order of 10^3-10^4 K/s **[12]**. This implies that the IPG glass phase is stable compared to metallic glass phase, *i.e.*, large amount of energy will be required to recrystallize the IPG.

During ion irradiation (which is a non-equilibrium process), the quenching rate of the thermal spike is so high (10^{12}-10^{15} K/s) that it becomes difficult to achieve short-range order in the damage cascade **[13]**. Hence, the possibility of spontaneous crystallization is ruled out. The role of impurity atoms in the crystallization process (heterogeneous nucleation) is ruled out due to self ion (O^+) irradiation.

Stress driven crystallization in amorphous materials has been reported recently **[14, 15]**. Specifically, shear band induced nanocrystallization in bulk metallic glasses is reported by Rizza et al **[16]**.

SRIM calculations show that in the case of 4 MeV O^+ ions in IPG, the nuclear energy loss (S_n ~5.5 eV/nm) is negligible compared to the electronic energy loss (S_e ~1.67 keV/nm). So the prominent mode of transfer of energy from the ion beam to the sample is by electronic energy loss. The

kinetic energy due to electronic energy loss is deposited exclusively by means of excitation and ionization of the electronic system of the solid. Further, the rapid energy transfer from the ion irradiation abnormally excites along the ion path whereas the surrounding is relatively at low temperature. The pressure wave formed in the wake of the projectile ion can generate an outgoing transient stress and strain. When the stress within an amorphous material increases beyond a critical value, shear bands are formed. Shear bands contain homogenously distributed excess free volume. The excess free volume is the analogue of vacancies in crystalline materials **[15]** and the excess free volume controls the diffusion rate in amorphous materials. This enhances atomic mobility and leads to increased short-range order and subsequent nucleation at longer time scales.

For more quantitative approach, the effect of the single ion induced local stress can be estimated, using the visco-elastic model **[17, 18],** to be

$$\sigma_{track} = \frac{(1+2\nu)}{2(1-\nu)(5-4\nu)} E\alpha\Delta T^{*} \sim 700 MPa$$

where, E= 72.3GPa is the Young's modulus, ν=0.24 is the Poisson ratio, α=4.1×10^{-5} K^{-1} is the linear thermal expansion co-efficient of IPG and ΔT^{*}~10^{3} K is the effective temperature of the ion track. The stress around the ion track is larger than the yield strength of glasses (typically 70 MPa) **[19]**, hence, the surrounding matrix undergoes substantial deformation resulting in shear band formation. Nanocrystals could have been nucleated in the vicinity of shear bands induced during thermal spike process.

Conclusion

The effect of ion irradiation on iron phosphate glass is studied using transmission electron microscopy. The electron diffraction patterns and HRTEM images confirm the presence of nanocrystals containing Fe, P and O in ion irradiated samples. Crystallization is observed even at low ion fluence (5×10^{13} ions/cm^{2}). In the present experiments, stress driven crystallization mechanism was invoked. The stress around the ion track is larger than the yield strength of the glass and hence, the surrounding matrix undergoes substantial deformation resulting in the formation of shear bands. Nanocrystals could have been nucleated in the vicinity of shear bands induced during thermal spike process.

Acknowledgements
UGC-DAE-CSR Kalpakkam node is acknowledged for the High Resolution TEM facility.

Reference

1. Donald L.W.; Metcalfe B.L.; Taylor R.N. *J. Mater. Sci.* **1997,** *32*, 5851. **DOI:** 10.1023/A:1018646507438
2. Kitheri Joseph; Asuvathraman R.; Venkata Krishnan R.; Ravindran T.R.; Govindaraj R.; Govindan Kutty K.V.; Vasudeva Rao P.R. *J. Nucl. Mater.* **2014** *452*, 273. **DOI:** 10.1016/j.jnucmat.2014.05.038
3. Weber W.J.; Ewing R.C.; Angell C.A.; Arnold G.W.; Cormack A.N.; Delaye J.M.; Griscom D.L.; Hobbs L.W.; Navrotsky A.; Price D.L.; Stoneham A.M.; Weinberg M.C. *J. Mater. Res.* **1997,** *12*, 1946. **DOI:** 10.1557/JMR.1997.0266
4. Sun K.; Ding T.; Wang L.M.; Ewing R.C.; Mat. Res. Soc. Symp. Proc. **2004**, *792*, R3.21.1. **DOI:** 10.1557/PROC-792-R3.21
5. Awazu K.; Roorda S.; Brebner J.L.; Ishii S.; Shima K. *Jpn. J. Appl. Phys.* **2003,** *42*, 3950. **DOI:** 10.1143/JJAP.42.3950
6. Kitheri Joseph; Ghosh S.; Govindan Kutty K.V.; Vasusdeva Rao P.R. *J. Nucl. Mater.* **2012**, *426*, 233. **DOI:** 10.1016/j.jnucmat.2012.03.048
7. The Stopping and Range of Ions in Matter (SRIM) simulation. **URL:**www.srim.org
8. **URL:** http://rsb.info.nih.gov/ij/
9. Liying Zhang; Mark E. Schlesinger; Richard K. Brow *J. Am. Ceram. Soc.* **2011**, *94*, 1605. **DOI:** 10.1111/j.1551-2916.2010.04287.x
10. Kitheri Joseph; Venkata Krishnan R.; Govindan Kutty K.V.; Vasudeva Rao P.R. *Thermochim. Acta* **2011**, *512*, 67. **DOI:** 10.1016/j.tca.2010.09.001
11. Kitheri Joseph; Asuvathraman R.; Venkata Krishnan R.; Ravindran T.R.; Govindaraj R.; Govindan Kutty K.V.; Vasudeva Rao P.R. *J. Nucl. Mater.* **2014**, *452*, 273. **DOI:** 10.1016/j.jnucmat.2014.05.038
12. Carter J.; Fu E.G.; Martin M.; Xie G.; Zhang X.; Wang Y.Q.; Wijesundera D.; Wang X.M.; Chu W.K.; Shao L. *Scripta Mater.* **2009**, *61*, 265. **DOI:** 10.1016/j.scriptamat.2009.03.060
13. Toulemonde M.; Dufour C.; Paumier E. *Phys. Rev. B* **1992** *46*, 14362. **DOI:** 10.1103/PhysRevB.46.14362
14. Matthews D.T.A.; Ocelik V.; Bronsveld P.M.; De Hosson J.Th.M. *Acta Mater.* **2008**, *56*, 1762. **DOI:** 10.1016/j.actamat.2007.12.029
15. Shravana Katakam; Santhanakrishnan S.; Hitesh Vora; Jun Y. Hwang; Rajarshi Banerjee; Narendra B. Dahotre *Phil. Mag. Lett.* **2012**, *92*, 617. **DOI:** 10.1080/09500839.2012.704416
16. Rizza G.; Dunlop A.; Kopcewicz M. *Nucl. Instrum Meth. B* **2006,** 245, 130. **DOI:** 10.1016/j.nimb.2005.11.089
17. Trinkaus H.; Ryazanov A.I. *Phys. Rev. Lett.* **1995**, *74*, 5072. **DOI:** 10.1103/PhysRevLett.74.5072
18. Trinkaus H. *J. Nucl. Mater.* **1995**, *223*, 196. **DOI:** 10.1016/0022-3115(95)00013-5
19. Handbook of Glass Properties; Narottam P. Bansal; Doremus R. H. **ISBN:** 978-0-12-078140-9